Rat α- and β-Parvalbumins: Comparison of Their Pentacarboxylate and Site-Interconversion Variants†

Michael T. Henzl,* Sayeh Agah, and John D. Larson

Department of Biochemistry, University of Missouri−Columbia, Columbia, Missouri 65211

Received March 1, 2004; Revised Manuscript Received May 17, 2004

ABSTRACT: Introduction of a fifth carboxylate into the ligand array of the CD site (via the combined S55D and E59D mutations) or the EF site (G98D) of rat α-parvalbumin substantially increases divalent ion affinity. This behavior, in conflict with that seen in model peptide systems, agrees with existing data for rat β-parvalbumin [Henzl et al. (1996) *Biochemistry 35*, 5856−5869]. The complete analysis of the S55D/E59D double variant necessitated characterization of α E59D. Whereas the D59E mutation has minimal influence on β CD site affinity, E59D has a major impact on the α CD site, lowering the apparent association constant by a factor of 14. The thermodynamic consequences of exchanging the rat α CD and EF site ligand arrays, which differ at the $+z$ and $-x$ coordination positions, were also examined. When the α CD array is imported into the EF site, it acquires a low-affinity phenotype, in agreement with previous findings for β [Henzl et al. (1998) *Biochemistry 37*, 9101−9111]. However, when the EF ligand array is introduced into the α CD binding loop, it retains a high-affinity signature. This result, contrary to that observed in β, suggests that the influence of the parvalbumin CD site environment supersedes the intrinsic behavior of the ligand array, a conclusion further supported by the disparate impact of the β D59E and α E59D mutations.

Oscillating cytosolic Ca^{2+} levels regulate numerous biological processes, achieving specificity through location, amplitude, duration, and frequency (*1*). These Ca^{2+} signals are a product of numerous metal ion−protein interactions involving ion channels, ATP-driven Ca^{2+} pumps, and Ca^{2+}-binding proteins. Thus, a detailed appreciation of the underlying metal ion−protein interactions is vital to our understanding of Ca^{2+} signaling.

"EF-hand" proteins were the first intracellular Ca^{2+}-binding proteins identified and characterized (*2*, *3*). The EF-hand motif consists of a central metal ion-binding loop flanked by short helical elements. The liganding residues, positioned at the approximate vertices of an octahedron, are referenced by Cartesian axes. The side chains of loop residues 1, 3, 5, and 12 contribute the $+x$, $+y$, $+z$, and $-z$ ligands, respectively. A backbone carbonyl serves as the $-y$ ligand, and a water molecule commonly occupies the $-x$ position. The Ca^{2+} coordination geometry is in fact pentagonal bipyramidal, due to bidentate ligation by the $-z$ carboxylate.

Certain EF-hand proteins serve as Ca^{2+}-dependent regulatory proteins and others as cytosolic Ca^{2+} buffers. Mirroring this functional diversity, EF-hand proteins exhibit large variations in metal ion-binding properties. Measured Ca^{2+}-binding constants, for example, span 4 orders of magnitude (*4*). Whereas high-affinity sites display Ca^{2+}- and Mg^{2+}-binding constants exceeding 10^7 and 10^4 M^{-1}, respectively, the corresponding values for low-affinity sites are 10^5-10^6 and $<10^3$ M^{-1}. After more than 2 decades of inquiry, the structural basis for these variations is incompletely understood (for reviews, see refs *5* and *6*).

Parvalbumins are small (M_r 12000), vertebrate-specific EF-hand proteins believed to function as Ca^{2+} buffers (*7*, *8*). Containing two Ca^{2+}-binding sites, known as the CD and EF sites,[1] the parvalbumin (PV) molecule (Figure 1A) has long been a popular system for investigating structure−function relationships in EF-hand proteins. Beginning with the X-ray crystallographic structure of carp parvalbumin (*10*), which established the EF-hand structural paradigm, biophysical characterization of this protein family has contributed significantly to our knowledge of EF-hand structure−affinity correlations.

The PV family includes α and β sublineages (*11*, *12*). α and β isoforms can be distinguished on the basis of isoelectric point ($\beta < 5$), C-terminal helix length (generally one residue longer for α), and lineage-specific residues (e.g., Cys-18 in β). The mammalian genome encodes one isoform from each lineage (*13*).

† This work was supported by NSF Awards MCB9603877 and MCB0131166 (to M.T.H.).

* Corresponding author. Tel: 573-882-7485. Fax: 573-884-4812. E-mail: henzlm@missouri.edu.

[1] Abbreviations: CD site, parvalbumin metal ion-binding site flanked by the C and D helical segments; DSC, differential scanning calorimetry; EDTA, ethylenediaminetetraacetic acid; EF site, parvalbumin metal ion-binding site flanked by the E and F helical segments; EGTA, ethylene glycol bis(β-aminoethyl ether)-*N*,*N*,*N*′,*N*′-tetraacetic acid; FAAS, flame atomic absorption spectrometry; Hepes, 4-(2-hydroxyethyl)-1-piperazineethanesulfonic acid; ITC, isothermal titration calorimetry; NLLS, nonlinear least squares; NTA, nitrilotriacetic acid; P_i, phosphate; PV, parvalbumin; RLC, myosin regulatory light chain; SDS−PAGE, sodium dodecyl sulfate−polyacrylamide gel electrophoresis.

10.1021/bi049582d CCC: $27.50
Published on Web 06/26/2004

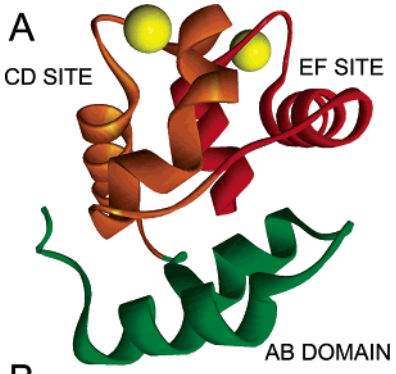

B

CD SITE

	51									60
β	D	**N**	D	**Q**	S	G	**Y**	**L**	**D**	**G**	D	E
α	D	**K**	D	**K**	S	G	**F**	**I**	**E**	**E**	D	E
	x		*y*		*z*		*-y*		*-x*		*-z*	

EF SITE

	90									100
β	D	**N**	D	G	D	G	K	I	**A**	**D**	E
α	D	**K**	D	G	D	G	K	I	**V**	**E**	E
	x		*y*		*z*		*-y*		*-x*		*-z*	

FIGURE 1: (A) Parvalbumin tertiary structure. Ribbon diagram for rat β, emphasizing the two-domain structure. The AB domain is shown in green, the CD site in orange, and the EF site in red. Produced with the atomic coordinates from ref *9*. (B) Amino acid sequences of the CD and EF binding loops in rat α- and β-parvalbumins. Nonidentities are shown in boldface type. The sequence data are from refs *19* and *20*, respectively.

Sequence data for the CD and EF sites of rat α- and β-parvalbumin are compared in Figure 1B. With the exception of the $-x$ position in the CD site, the coordinating residues are identical in the two proteins. Nevertheless, they exhibit very distinct metal ion-binding properties. Whereas the α CD and EF sites behave equivalently in divalent ion-binding assays, displaying a high-affinity phenotype (*14*−*16*), the two sites in β are decidedly nonequivalent. Although the EF site is a typical high-affinity site, the CD site exhibits a low-affinity signature (*17*, *18*). This disparity in metal ion-binding behavior, in proteins exhibiting 49% overall sequence identity, provides a useful system for examining the influence of protein architecture on divalent ion affinity.

In EF-hand peptide analogues, Ca^{2+} affinity is maximal in sites containing four carboxylate ligands positioned along the $+x$, $-x$ and $+z$, $-z$ axes (*21*−*24*). Addition of a fifth carboxylate lowers metal ion affinity, presumably due to increased interligand repulsion (*25*). However, introduction of a fifth carboxylate ligand into either binding site in rat β significantly raises Ca^{2+} affinity in the mutated site (*26*). In the CD site, replacement of Ser-55 by aspartate (S55D) increases the apparent Ca^{2+}-binding constant for that site from 1.5×10^6 to 1.6×10^7 M^{-1}. Replacement of Gly-98 in the EF site by aspartate (G98D) increases the apparent binding constant from 2.2×10^7 to 2.5×10^8 M^{-1}. Because these mutations add a potential fifth carboxylate to the coordination sphere of the bound metal ion, the resulting proteins are referred to as "pentacarboxylate" variants. The various ligand constellations discussed in this paper are depicted schematically in Figure 2.

As part of an inquiry into the nonequivalence of the β-PV CD and EF sites, "site-interconversion" variants were also produced, in which the CD and EF ligand arrays had been interchanged (*27*). The combined S55D/D59G mutations, within the CD site, create a version of the protein having, in effect, two EF site ligand arrays. Interestingly, these mutations have little impact on the apparent Ca^{2+} affinity of the CD site, the engineered CD site exhibiting Ca^{2+} affinity comparable to the wild-type β CD site. The combined D94S/G98D mutations, within the EF site, create a protein having two CD-like ligand arrays. Interestingly, the quasi-CD site resulting from these mutations displays markedly reduced affinity for Ca^{2+}.

Because the rat β-parvalbumin isoform has an unusually high net charge (approximately −15) and atypical divalent ion-binding properties, it was of interest to examine the pentacarboxylate and site-interconversion mutations in a more typical parvalbumin background. The rat α isoform was a logical choice for this study, given its lower net charge (approximately −5) and much higher divalent ion affinity.

MATERIALS AND METHODS

Protein Purification. Site-specific variants of rat α and β were expressed in *Escherichia coli* and isolated using procedures described previously for the wild-type proteins (*17*, *28*). Concentrations were determined spectrophotometrically, employing molar extinction coefficients of 1600 M^{-1} cm^{-1} for α and 3260 M^{-1} cm^{-1} for β. The absence of tryptophan in β, and both tyrosine and tryptophan in α, permits a spectrophotometric evaluation of homogeneity. Assuming an average mass extinction coefficient of 0.5 cm^{-1} $(mg/mL)^{-1}$ at 292 nm for tryptophan, the purity of all preparations exceeded 98%. The absence of proteolytic degradation was confirmed by SDS−PAGE.

Site-specific mutations were introduced by oligonucleotide-directed mutagenesis, using either the Transformer (Clontech) or Quik-Change (Stratagene) kit. Each variant was sequenced to verify the fidelity of the PV coding regions.

Ca^{2+}-Binding Assays. Divalent metal ions were removed from the proteins and buffers, prior to analysis, by EDTA−agarose chromatography at 4 °C. The chelating matrix was prepared by carbodiimide-promoted coupling of Na_2EDTA to (aminohexyl)agarose at pH 6.0, as described elsewhere (*29*). The Ca^{2+}-binding capacity of the resulting material is 25−30 μmol/mL of gel. Typically, 1−2 mL of resin is used for each milligram of protein loaded, and elution is performed at 0.5 mL/min. In every case, the residual Ca^{2+} content following this treatment, measured by flame atomic absorption, was less than 0.02 molar equiv.

$^{45}Ca^{2+}$ flow dialysis (*30*) was used to measure the Ca^{2+} affinities of α S55D, α S55D/E59G, α D94S/G98D, α D94S/G98E, and β G98E. To facilitate comparison with results previously published for rat β (*17*, *26*, *27*), the data were collected in 0.15 M NaCl and 0.025 M Hepes−NaOH, pH 7.4. Nonlinear least-squares analyses were performed with Origin v.5.0 (OriginLab), fitting the data to a two-site Adair equation:

$$\bar{X} = \frac{K_1[Ca^{2+}] + 2K_2K_1[Ca^{2+}]^2}{1 + K_1[Ca^{2+}] + K_2K_1[Ca^{2+}]^2} \quad (1)$$

where $\bar{X}$ is the number of equivalents of Ca^{2+} bound and K_1 and K_2 are the two macroscopic association constants.

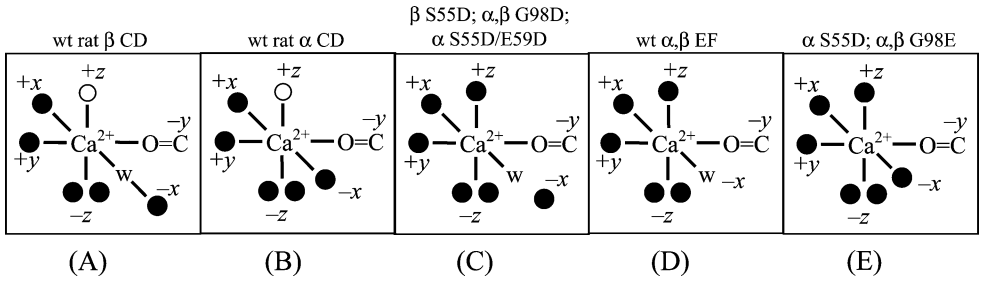

FIGURE 2: Ligand arrays from wild-type and pentacarboxylate sites. Solid circles (●) denote carboxylate oxygen atoms; the open circles (○) denote the serine hydroxyl; w indicates a water molecule. (A) The CD site from wild-type rat β-PV; (B) the CD site from wild-type rat α; (C) ligand array for the CD site in either β S55D or α S55D/E59D or the EF site in G98D (α or β); (D) the EF site from either wild-type α or β; (E) ligand array in either the CD site of α S55D or the EF site of G98E (α or β).

The Ca^{2+}- and Mg^{2+}-binding affinities of α S55D/E59D and α G98D were determined by global analysis of ITC data in 0.15 M NaCl and 0.025 M Hepes, pH 7.4. Titrations were conducted with Ca^{2+}, with Mg^{2+}, with Ca^{2+} in the presence of fixed levels of Mg^{2+}, with Ca^{2+} in the presence of EDTA, with Ca^{2+} in the presence of EGTA, and with Mg^{2+} in the presence of EDTA. The resulting composite data set was subjected to NLLS analysis, evaluating parameter uncertainties by Monte Carlo analysis, as described elsewhere (*31*).

The Ca^{2+}-binding properties of α G98E and α E59D were determined by global ITC analysis, using abbreviated protocols. The α E59D study included a titration in the presence of 10 mM citrate. The Ca^{2+}-binding constant for citrate (1670 M^{-1}) was estimated from the decrease in EDTA Ca^{2+} affinity observed in the presence of citrate. The apparent enthalpy of Ca^{2+} binding for citrate is very small, under the chosen solution conditions, and was included as an adjustable parameter in the global fit. The Ca^{2+} affinity of β D94S/G98E was estimated from single ITC experiments.

All of the variant proteins were studied at 25 °C, with the exception of α S55D/E59D and α G98D. As discussed elsewhere (*31*), the latter are partially unfolded at 25 °C, a consequence of their low conformational stabilities. To eliminate this complication, the divalent ion affinities of S55D/E59D and α G98D were measured at 5 °C.

Where data are available for both methods, flow-dialysis and ITC-based analyses yield comparable estimates of the binding constants (*31*, *32*).

Calorimetry. Isothermal titration calorimetry (ITC) experiments were performed at 25 °C, either with a Model 4209 isothermal titration calorimeter from Calorimetry Sciences Corp. (CSC) or with a VP-ITC (MicroCal). Data collected with the CSC calorimeter were analyzed with BindWorks v.1.0 (Applied Thermodynamics), supplying estimates of the binding constants determined by flow dialysis. Origin v.5.0 was used for integration of the raw VP-ITC data and for analysis of individual titrations, using the curve-fitting modules supplied with the instrument.

Differential scanning calorimetry (DSC) was performed in a modified Nano DSC calorimeter (Calorimetry Sciences Corp.), equipped with cylindrical sample cells (0.32 mL active volume). Prior to analysis, samples were dialyzed to equilibrium against 0.20 M NaCl, 0.010 M sodium phosphate, and 0.005 M EDTA, pH 7.4. An aliquot of the dialysis reservoir served as the reference buffer. A scan rate of 1.0 deg/min was employed for all experiments. To confirm that the thermal denaturation events were thermodynamically reversible under the chosen experimental conditions, samples of the proteins were heated, cooled, and then reheated. In every case, an endotherm was observed on the rescan, comparable in area to the original.

DSC data analysis was performed with CpCalc v.2.1 (Applied Thermodynamics), and the reported uncertainties in T_m and ΔH_d reflect the standard deviations for at least three determinations.

The ensuing discussion contains references to both microscopic (k_1, k_2) and macroscopic (K_1, K_2) Ca^{2+}-binding constants. Whereas microscopic (or site-specific) constants reflect the affinities of discrete binding sites, macroscopic constants reflect the average affinities associated with the binding events. In the absence of positive cooperativity, the macroscopic constants are mathematically related to the microscopic binding constants as follows:

$$K_1 = k_1 + k_2 \qquad K_2 = k_1k_2/(k_1 + k_2) \tag{2}$$

Conversely, given values for K_1 and K_2, the apparent values of k_1 and k_2 are equal to

$$k_1 = \frac{K_1 + \sqrt{K_1^2 - 4K_1K_2}}{2}$$

$$k_2 = \frac{K_1 - \sqrt{K_1^2 - 4K_1K_2}}{2} \tag{3}$$

RESULTS

Pentacarboxylate Variants. In the following paragraphs, thermal stability and Ca^{2+}-binding data are presented for the S55D, S55D/E59D, G98D, and G98E variants of rat α and for the G98E variant of rat β. These data are summarized in Tables 1 and 2, respectively. Mg^{2+}-binding constants are also reported for α S55D/E59D and α G98D and are listed in Table 3. The analysis of the S55D mutation in α S55D/E59D necessitated production and characterization of the α E59D variant, and the properties of α S55D/E59D are discussed with respect to both wild-type α and α E59D.

Intrinsic Thermal Stability. The relative conformational stabilities of the various proteins were examined by DSC. Representative scans are presented in Figure 3A for the E59D (◇), S55D (□), S55D/E59D (△), G98D (○), and G98E (▽) variants of rat α, along with data for the wild-type protein (●). Data for the relevant β variants, D59E (◇), S55D (△), G98D (○), and G98E (▽), and wild type (●) are presented in Figure 3C.

Table 1: Relative Stabilities of Rat α- and β-Parvalbumin Variants

protein	T_m[a] (°C)	$\Delta\Delta T_m$ (°C)	$\Delta\Delta G_{conf}$[b] (kcal/mol)	protein	T_m (°C)	$\Delta\Delta T_m$ (°C)	$\Delta\Delta G_{conf}$[b] (kcal/mol)
wt rat α[c]	45.8 (0.2)			wt rat β[c]	53.6 (0.2)		
α S55D	34.6 (0.3)	−11.2	−2.2	β S55D	49.3 (0.2)	−4.3	−1.0
α E59D	49.8 (0.2)	4.0	0.8	β D59E	54.8 (0.2)	1.2	0.3
α S55D/E59D	37.3 (0.3)	−8.5	−1.7				
α G98D	43.2 (0.2)	−2.6	−0.5	β G98D	51.8 (0.2)	−1.8	−0.4
α G98E	32.4 (0.3)	−13.4	−2.7	β G98E	48.8 (0.2)	−4.8	−1.1
α S55D/E59G	41.6 (0.2)	−4.2	−0.8	β S55D/D59G	51.3 (0.2)	−2.3	−0.5
α D94S/G98D	51.2 (0.4)	5.4	1.1	β D94S/G98D	55.0 (0.2)	1.4	0.3
α D94S/G98E	42.5 (0.3)	−3.3	−0.6	β D94S/G98E	52.4 (0.2)	−1.2	−0.3

[a] Uncertainties are given in parentheses. [b] The alteration in the free energy change accompanying denaturation, calculated from the $\Delta\Delta T_m$ values, using eq 4. [c] Reference *38*.

Table 2: Summary of the Ca^{2+}-Binding Properties for the α and β Pentacarboxylate and Site-Interconversion Variants

protein	temp (°C)	K_1 (M^{-1})	ΔH_1 (kcal/mol)	K_2 (M^{-1})	ΔH_2 (kcal/mol)	ΔG_{Ca}[a] (kcal/mol)	ΔH_{Ca}[b] (kcal/mol)	$-T\Delta S_{Ca}$[b] (kcal/mol)	$\Delta\Delta G_{Ca}$ (kcal/mol)	$\Delta\Delta H_{Ca}$ (kcal/mol)	$-T\Delta\Delta S_{Ca}$ (kcal/mol)
rat α-PV[c]	25	$2.5(0.2)\times10^8$	−1.3(0.1)	$6.2(0.2)\times10^7$	−4.3(0.1)	−22.0	−5.6	−16.4			
rat α-PV[c]	5	$2.6(0.2)\times10^8$	−1.4(0.1)	$6.4(0.2)\times10^7$	−4.0(0.1)	−20.5	−5.5	−15.1			
α S55D	25	$2.1(0.2)\times10^8$	−6.3(0.3)	$5.0(0.2)\times10^7$	−2.4(0.2)	−21.8	−8.7	−13.1	0.2	−3.1	3.3
α E59D	25	$1.2(0.1)\times10^8$	−4.5(0.1)	$7.8(0.3)\times10^6$	−1.6(0.1)	−20.3	−6.1	−14.2	1.7	−0.5	2.2
α S55D/E59D[d]	5	$1.9(0.3)\times10^9$	−4.8(0.2)	$2.5(0.4)\times10^8$	−4.4(0.2)	−24.0	−9.2	−14.8	−2.0	−3.6	1.6
α G98D	5	$1.2(0.2)\times10^9$	−4.6(0.1)	$7.7(0.2)\times10^7$	−2.6(0.1)	−23.1	−7.2	−15.9	−1.1	−1.6	0.5
α G98E	25	$4.4(0.3)\times10^8$	−15.6(0.2)	$5.3(1.0)\times10^7$	−1.3(0.2)	−22.2	−16.9	−5.3	−0.2	−11.3	11.1
α S55D/E59G	25	$2.4(0.2)\times10^8$	−3.8(0.2)	$2.9(0.2)\times10^7$	−2.3(0.2)	−21.5	−6.1	−15.4	0.5	−0.5	1.0
α D94S/G98D	25	$9.7(0.2)\times10^7$	−2.8(0.1)	$4.4(0.1)\times10^5$	1.7(0.1)	−18.5	−1.1	−17.4	3.5	4.5	−1.0
α D94S/G98E	25	$5.5(0.2)\times10^7$	−2.1(0.1)	$4.7(2.0)\times10^5$	1.4(0.1)	−18.2	−0.7	−17.5	3.8	4.9	−1.1
rat β-PV[c]	25	$2.4(0.1)\times10^7$	−4.1(0.1)	$1.4(0.1)\times10^6$	−3.5(0.1)	−18.4	−7.6	−10.8			
β S55D[e]	25	$5.3(0.1)\times10^7$	−6.7(0.1)	$1.1(0.1)\times10^7$	−2.4(0.1)	−20.1	−9.1	−11.0	−1.7	−1.5	−0.2
β D59E[f]	25	$2.6(0.1)\times10^7$	−5.8(0.1)	$1.7(0.1)\times10^6$	−1.1(0.1)	−18.5	−6.9	−11.6	−0.1	0.7	−0.8
β G98D[e]	25	$2.5(0.2)\times10^8$	−4.0(0.1)	$1.2(0.1)\times10^6$	−3.4(0.1)	−19.7	−7.4	−12.3	−1.3	0.2	−1.5
β G98E	25	$5.9(0.1)\times10^7$	−7.0(0.2)	$1.1(0.1)\times10^6$	−2.1(0.2)	−18.7	−9.1	−9.6	−0.3	−1.5	1.2
β S55D/D59G[g]	25	$2.3(0.1)\times10^7$	−5.1(0.1)	$1.3(0.1)\times10^6$	−0.3(0.3)	−18.3	−5.4	−12.9	0.1	2.2	−2.1
β D94S/G98D[g]	25	$4.3(0.1)\times10^6$	−2.8(0.1)	$3.2(0.1)\times10^5$	−0.8(0.1)	−16.5	−3.6	−12.9	1.9	4.0	−2.1
β D94S/G98E	25	$1.1(0.1)\times10^6$	−2.8(0.1)	$3.1(0.1)\times10^5$	1.8(0.1)	−15.7	−1.0	−14.7	2.7	6.6	−3.9

[a] Total apparent standard free energy of Ca^{2+} binding, calculated with the relationship $\Delta G = -RT\ln(K_1K_2)$. [b] Calculated with the relationship $\Delta G = \Delta H - T\Delta S$. [c] Reference *32*. [d] Reference *31*. [e] Reference *26*. [f] Reference *17*. [g] Reference *27*.

Table 3: Mg^{2+}-Binding Behavior of the α and β Pentacarboxylate Variants

protein	temp (°C)	K_{1M} (M^{-1})	ΔH_{1M} (kcal/mol)	K_{2M} (M^{-1})	ΔH_{2M} (kcal/mol)	ΔG_{Mg}[a] (kcal/mol)	ΔH_{Mg}[b] (kcal/mol)	$-T\Delta S_{Mg}$[b] (kcal/mol)	$\Delta\Delta G_{Mg}$ (kcal/mol)	$\Delta\Delta H_{Mg}$ (kcal/mol)	$-T\Delta\Delta S_{Mg}$ (kcal/mol)
rat α-PV[c]	5	$1.8(0.1)\times10^4$	7.8(0.1)	$4.3(0.2)\times10^3$	1.6(0.1)	−10.0	9.4	−19.4			
α S55D/E59D[d]	5	$2.7(0.4)\times10^5$	3.1(0.1)	$1.9(0.3)\times10^4$	4.3(0.1)	−12.3	7.4	−19.7	−2.3	−2.0	−0.3
α G98D	5	$3.1(0.2)\times10^4$	4.9(0.1)	$3.3(0.2)\times10^3$	4.8(0.1)	−10.2	9.7	−19.9	−0.2	0.3	−0.5
rat β-PV[d]	25	$9.4(0.3)\times10^3$	3.0(0.1)	$1.6(0.2)\times10^2$	4.2(0.2)	−8.4	7.2	−15.6			
β S55D[e]	25	4.5×10^4	nd	8.3×10^3	nd	−11.6			−3.2		
β G98D[e]	25	8.0×10^3	nd	2.6×10^2	nd	−8.6			−0.2		

[a] Total apparent standard free energy of Mg^{2+} binding, calculated with the relationship $\Delta G = -RT\ln(K_1K_2)$. [b] Calculated with the relationship $\Delta G = \Delta H - T\Delta S$. [c] Reference *32*. [d] Reference *31*. [e] Reference *26*.

Introduction of a potential fifth carboxylate ligand into the coordination sphere destabilizes the Ca^{2+}-free proteins. In α, G98E has the greatest impact ($\Delta T_m = -13.4°$), followed by S55D ($\Delta T_m = -11.2°$), then S55D/E59D ($\Delta T_m = -8.5°$), and G98D ($\Delta T_m = -2.6°$). The corresponding β variants exhibit the same pattern of destabilization: G98E ($\Delta T_m = -4.8°$) > S55D ($\Delta T_m = -4.3°$) > G98D ($\Delta T_m = -1.8°$). However, the ΔT_m values are significantly larger for the α series.

The most obvious difference in the Ca^{2+}-coordination chemistries of rat α and β occurs at the $-x$ position in the CD site. Whereas residue 59 is glutamate in α, it is aspartate in β. Prior to the cloning of the proteins, there was speculation that this single difference was primarily responsible for the attenuated divalent ion affinity of the β CD site. The identity of this residue has a differential impact on the stabilities of α and β. The D59E mutation modestly increases the stability of β, raising the T_m by 1.2 deg. By contrast, the converse mutation in α E59D, raises the melting temperature by 4.0 deg.

Assuming that the change in heat capacity upon denaturation for the variant proteins is comparable to that of the wild-type protein, the alteration in conformational stability ($\Delta\Delta G_{conf}$) resulting from each mutation can be estimated from the shift in melting temperature, using this approximation:

$$\Delta\Delta G_{conf} = \frac{\Delta T_m \Delta H_d}{T_m} \quad (4)$$

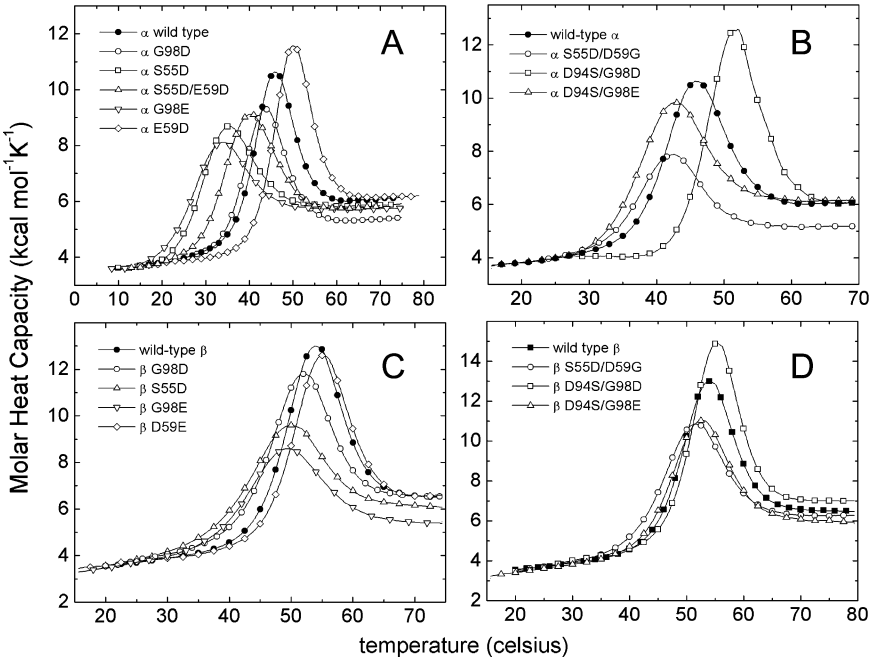

FIGURE 3: Differential scanning calorimetry analyses. (A) Rat α pentacarboxylate variants: wild-type α (●), G98D (○), S55D (□), S55D/E59D (△), G98E (▽), and E59D (◇). (B) Rat α site-interconversion variants: wild-type α (●), S55D/E59G (○), D94S/G98D (□), and D94S/G98E (△). (C) Rat *β* pentacarboxylate variants: wild-type *β* (●), G98D (○), S55D (△), G98E (▽), and D59E (◇). (D) Rat *β* site-interconversion variants: wild-type *β* (●), S55D/D59G (○), D94S/G98D (□), and D94S/G98E (△). Protein concentrations for these experiments ranged between 4 and 7 mg/mL.

where T_m and ΔH_d are the melting temperature and denaturational enthalpy for the wild-type protein and ΔT_m is the change in melting temperature resulting from the mutation (*33*). Because ΔG_{conf} represents the free energy change accompanying denaturation, positive values of $\Delta\Delta G_{conf}$ correspond to stabilization of the native state, and negative values correspond to destabilization. The calculated $\Delta\Delta G_{conf}$ values are listed in Table 1 and plotted in Figure 4A. As discussed below, α S55D/E59D, α G98D, *β* S55D, and *β* G98D exhibit substantial increases in Ca^{2+} affinity. Significantly, the Ca^{2+}-free states of these four proteins suffer perceptible decreases in conformational stability. Conversely, α E59D exhibits decreased Ca^{2+} affinity and a significant increase in ΔG_{conf}.

Ca^{2+} affinities were measured at pH 7.4 in Hepes-buffered NaCl. The binding constants for several of the proteins discussed in this paper were determined by flow dialysis. Representative binding curves, and the optimal NLLS fits, are displayed for α S55D (Figure 5A, ●) and for *β* G98E (Figure 5B, ●).

The Ca^{2+} affinities of α S55D/E59D and α G98D proved too high to unambiguously measure by flow dialysis and were determined instead by global analysis of ITC data, as described in Materials and Methods. The integrated data for the various experiments on α G98D are displayed in Figure 6, the solid lines through the data points indicating the best least-squares fit to the composite data set. Corresponding data for α S55D/E59D have been published elsewhere (*31*).

The Ca^{2+}-binding constants for αE59D and α G98E were also estimated by global analysis of ITC data, employing a smaller number of experiments. The integrated data and best NLLS fits are displayed in panels A and B of Figure 7, respectively.

Macroscopic stepwise binding constants and estimates of the corresponding overall free energy changes are tabulated for each protein in Table 2. The changes in the overall thermodynamic parameters for Ca^{2+} binding ($\Delta\Delta G_{Ca}$, $\Delta\Delta H_{Ca}$, and $-T\Delta\Delta S_{Ca}$), relative to the wild-type proteins, are plotted in panels B−D of Figure 4. G98D has a similar impact on overall Ca^{2+} affinity in α and *β*. In the α isoform, the

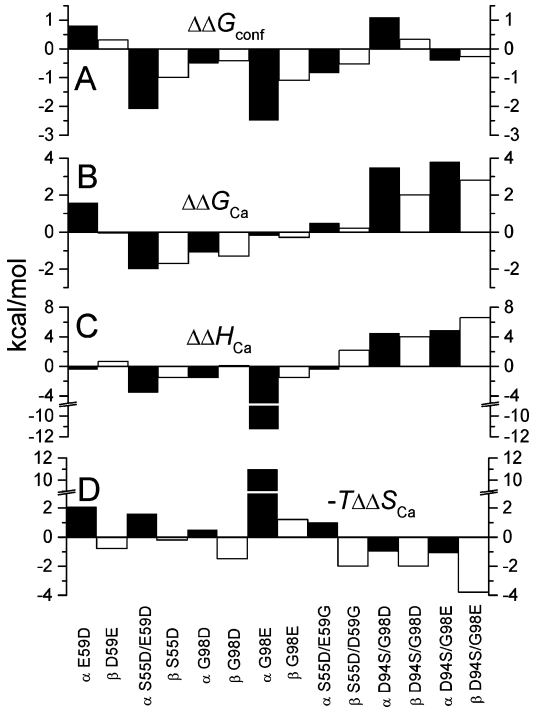

FIGURE 4: Thermodynamic comparison of the variant proteins. (A) Alterations in conformational stability, $\Delta\Delta G_{conf}$. (B) Alterations in apparent total standard free energy for Ca^{2+} binding, $\Delta\Delta G_{Ca}$. (C) Alterations in the enthalpic contribution to the Ca^{2+}-binding free energy, $\Delta\Delta H_{Ca}$. (D) Alterations in the entropic contribution to the Ca^{2+}-binding free energy, $-T\Delta\Delta S_{Ca}$. To facilitate comparison, the corresponding α and *β* variants are displayed side by side.

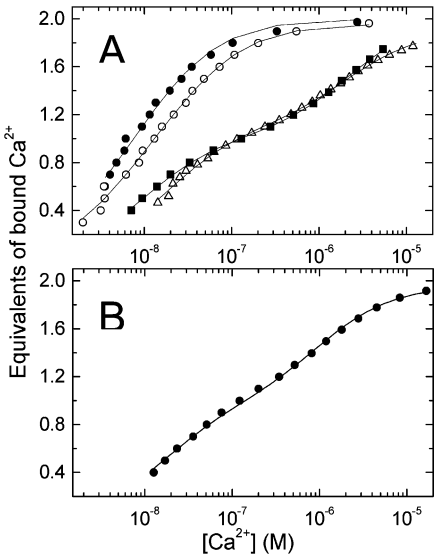

FIGURE 5: $^{45}Ca^{2+}$ flow-dialysis measurements. (A) Binding data for α S55D (●), α S55D/E59G (○), α D94S/G98D (■), and α D94S/G98E (△). (B) Data for *β* G98E (●).

mutation raises K_1 by a factor of 4.6, from 2.6×10^8 to 1.2×10^9 M^{-1}. K_2 is increased by 20%, from 6.4×10^7 to 7.7×10^7 M^{-1}. In *β*, K_1 increases by a factor of 10, from 2.4×10^7 to 2.5×10^8 M^{-1}, and K_2 decreases slightly, from 1.4×10^6 to 1.2×10^6 M^{-1}.

The G98E mutation likewise has similar consequences in α and *β*, producing a significant increase in K_1 and a minor decrease in K_2. In α, K_1 increases by a factor of 1.8, to 4.4×10^8 M^{-1}, and K_2 decreases by 15%, to 5.3×10^7 M^{-1}. In *β*, K_1 increases by a factor of 2.5, to 5.9×10^7 M^{-1}, and K_2 decreases by 21%, to 1.1×10^6 M^{-1}.

The impact of the S55D mutation on the wild-type proteins is isoform-dependent. Whereas S55D improves the overall standard free energy change for Ca^{2+} binding in *β* by 1.7 kcal/mol, α S55D exhibits a minor decrease in Ca^{2+} affinity ($\Delta\Delta G = 0.2$ kcal/mol). K_1 and K_2 are reduced in the latter by 16% and 19%, respectively, to 2.1×10^8 and 5.0×10^7 M^{-1}. Recall that residue 59 occupies the $-x$ ligand position in the CD site. Whereas Glu-59 directly coordinates the bound Ca^{2+} in α, Asp-59 coordinates indirectly in *β*, via an intervening water molecule. Reasoning that this difference might underlie the disparate influence of the S55D mutation in α and *β*, the α S55D/E59D variant was prepared. The combined mutations should produce a coordination sphere in the α CD site identical to that in *β* S55D. Consistent with that expectation, α S55D/E59D likewise exhibits a large increase in Ca^{2+}. The apparent macroscopic association constants for Ca^{2+} increase by factors of 7.3 and 3.9, relative to wild-type α, to 1.9×10^9 and 2.5×10^8 M^{-1} (*31*).

Interestingly, comparison of α S55D/E59D and α E59D reveals that the S55D mutation has a greater impact on Ca^{2+} affinity in α than in *β*. When Ser-55 is replaced by aspartate in α E59D, K_1 and K_2 increase by factors of 16 and 32, respectively. The same mutation in rat *β* increases K_1 and K_2 by factors of 2.2 and 7.8.

The Ca^{2+}-binding behavior of α E59D merits comment. Although the sequence difference at residue 59, aspartate vs glutamate, was initially heralded as the explanation for the attenuated Ca^{2+} affinity of rat *β* (*34*), replacement of Asp-59 by glutamate (D59E) produces a very modest increase in the Ca^{2+} affinity of rat *β* (*17*, *35*). By contrast, the data presented here reveal that replacement of Glu-59 by aspartate dramatically reduces the Ca^{2+} affinity of rat α. K_1 and K_2 decrease by factors of 2.1 and 7.9, respectively, to 1.2×10^8 and 7.8×10^6 M^{-1}.

Ca^{2+}-binding enthalpies for each protein have been measured by ITC. The analyses of α E59D, α S55D/E59D, α G98D, and α G98E were discussed in the previous section. Figure 8 presents raw and integrated heat data for α S55D (panels A and B) and *β* G98E (panels C and D). The $\Delta\Delta H_{Ca}$ values resulting from all of these mutations are compared for α and *β* in Figure 4C. In α, G98E produces the largest change in binding enthalpy ($\Delta\Delta H_{Ca} = -11.3$ kcal/mol), followed by S55D/E59D ($\Delta\Delta H_{Ca} = -3.6$ kcal/mol), S55D ($\Delta\Delta H_{Ca} = -3.1$ kcal/mol), and G98D ($\Delta\Delta H_{Ca} = -1.6$ kcal/mol). This order parallels that observed for *β*.

Mg^{2+} Affinities. The global ITC analyses of α G98D and α S55D/E59D also yielded estimates of the Mg^{2+}-binding parameters, listed in Table 3. The combined S55D/E59D mutations substantially increase the Mg^{2+} affinity of the mutated site. Whereas wild-type α displays apparent macroscopic Mg^{2+}-binding constants of 1.8×10^4 and 4.3×10^3 M^{-1} at 5 °C, α S55D/E59D exhibits corresponding values of 2.7×10^5 and 1.9×10^4 M^{-1}. By contrast, the G98D mutation has a smaller, mixed impact on α Mg^{2+} affinity. The first macroscopic constant increases by 72%, to 3.1×10^4 M^{-1}; the second is reduced by 23%, to 3.3×10^3 M^{-1}.

Site-Interconversion Variants. The ligand arrays in the parvalbumin CD and EF sites differ at the $+z$ and $-x$ positions: serine and glutamate/aspartate in the CD site and aspartate and glycine in the EF site. Thus, if Ser-55 and Glu-59 are simultaneously replaced in rat α by aspartate and glycine (yielding α S55D/E59G), the CD site acquires an EF-like array. Conversely, if Asp-94 and Gly-98 are replaced by serine and glutamate (yielding α D94S/G98E), the EF site acquires a CD-like array. The thermodynamic consequences of these interconversions are examined in the following paragraphs. In rat *β*, residue 59 is aspartate rather than glutamate. Thus, for completeness, the α D94S/G98D and *β* D94S/G98E variants were also produced and characterized.

Intrinsic Stability. DSC data are presented in Figure 3B for α S55D/E59G (○), α D94S/G98D (□), and α D94S/G98E (△), together with corresponding data for wild-type α (●). Data for the corresponding *β* proteins are displayed in Figure 3D. The combined S55D and E59G mutations lower the transition temperature of the α isoform by 4.2 deg, from 45.8 to 41.6 °C. The combined D94S and G98D mutations raise the T_m by 5.4 deg, to 51.2 °C. These changes parallel those seen with the *β* isoforms (*27*). In contrast to D94S/G98D, the combined D94S and G98E mutations have a destabilizing effect, reducing the T_m of α by 3.3 deg to 42.5 °C. The *β* D94S/G98E variant likewise exhibits reduced stability, with a T_m (52.4 °C) 1.2 deg lower than wild-type *β*.

As described above, eq 4 can be used to estimate the change in conformational free energy resulting from the shift in T_m. The alterations resulting from the various mutations are depicted graphically in Figure 4A. Whereas α S55D/E59G and α D94S/G98E are destabilized by 0.8 and 0.6 kcal/mol, respectively, α D94S/G98D is stabilized by 1.1 kcal/

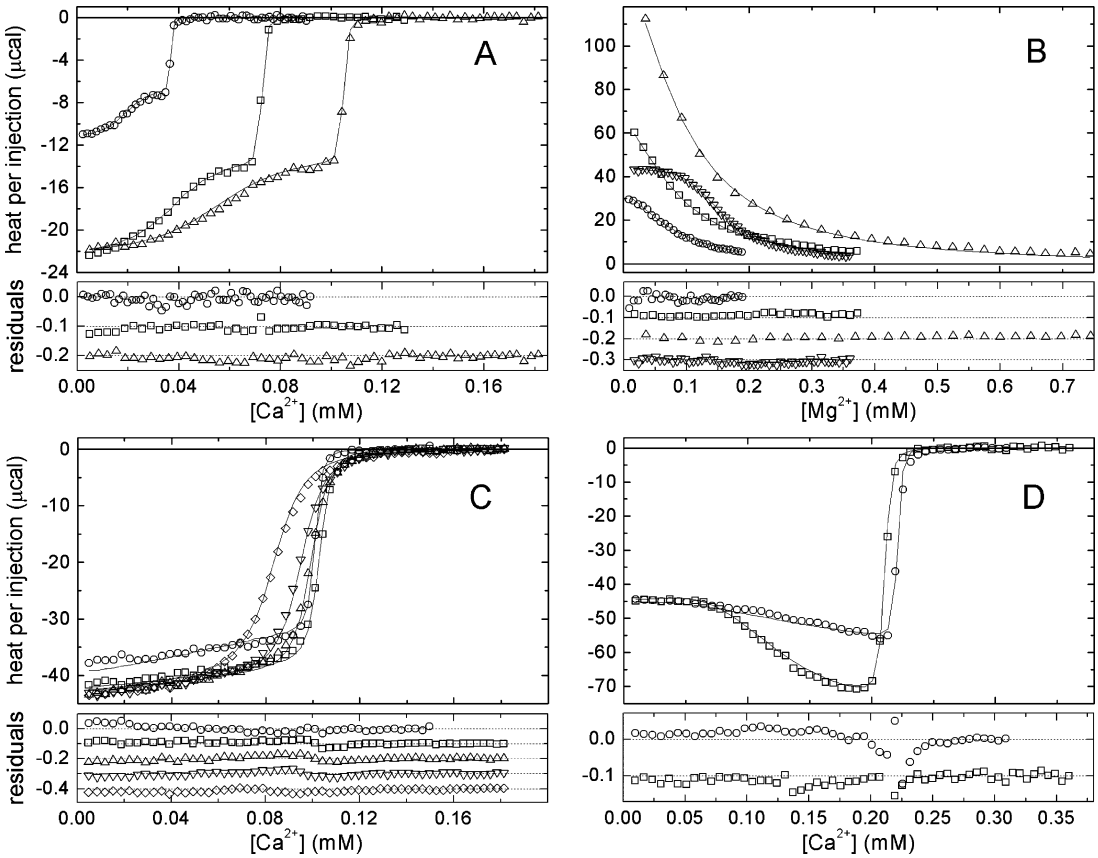

FIGURE 6: Global ITC analysis of α G98D divalent ion-binding properties. Integrated data, together with the best NLLS fits, are displayed in the upper panel; scaled residuals, offset for clarity, are displayed in the lower panel. (A) 0.50 mM Ca^{2+} vs 20 μM α G98D (○); 1.0 mM Ca^{2+} vs 40 μM α G98D (□); 1.0 mM Ca^{2+} vs 60 μM α G98D (△). (B) 1.0 mM Mg^{2+} vs 60 μM α G98D (○); 2.1 mM Mg^{2+} vs 60 μM α G98D (□); 4.1 mM Mg^{2+} vs 60 μM α G98D (△); 2.0 mM Mg^{2+} vs 60 μM α G98D, 0.12 mM EDTA (▽). (C) 1.0 mM Ca^{2+} vs 57 μM α G98D, 0.47 mM Mg^{2+} (○); 1.0 mM Ca^{2+} vs 59 μM α G98D, 2.1 mM Mg^{2+} (□); 1.0 mM Ca^{2+} vs 56 μM α G98D, 5.2 mM Mg^{2+} (△); 1.0 mM Ca^{2+} vs 53 μM α G98D, 10.3 mM Mg^{2+} (▽); 1.0 mM Ca^{2+} vs 46 μM α G98D, 20.6 mM Mg^{2+} (◇). (D) 2.0 mM Ca^{2+} vs 59 μM α G98D, 0.12 mM EDTA (○); 2.0 mM Ca^{2+} vs 59 μM α G98D, 0.12 mM EGTA (□).

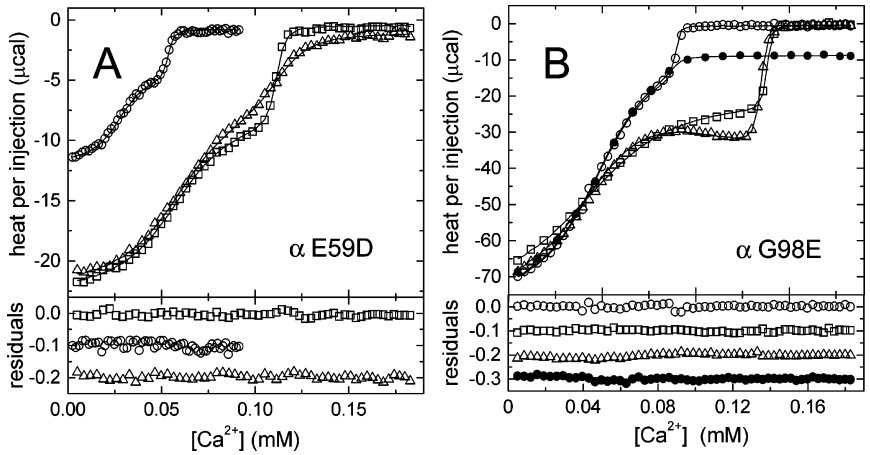

FIGURE 7: Determination of Ca^{2+} affinities of α E59D and α G98E by ITC. (A) E59D. Integrated data, together with the best least-squares fits, are displayed in the upper panel; scaled residuals are displayed in the lower panel. Key: 0.50 mM Ca^{2+} vs 30 μM α E59D (○); 1.0 mM Ca^{2+} vs 60 μM α E59D (□); 1.0 mM Ca^{2+} vs 60 μM α E59D, 10 mM citrate (△). (B) G98E. Integrated data with optimal fits are presented in the upper panel and scaled residuals in the lower. Key: 1.0 mM Ca^{2+} vs 49 μM α G98E (○); 1.0 mM Ca^{2+} vs 49 μM α G98E, 60 μM EDTA (□); 1.0 mM Ca^{2+} vs 48 μM α G98E, 60 μM EGTA (△); 1.0 mM Ca^{2+} vs 48 μM α G98E, 60 μM EGTA (△); 1.0 mM Ca^{2+} vs 48 μM α G98E, 1.0 mM NTA (●).

mol. The corresponding changes for the β proteins are −0.5, −0.3, and 0.3 kcal/mol.

Ca^{2+} Affinity. Binding data are presented in Figure 5A for α S55D/E59G (○), α D94S/G98D (■), and α D94S/G98E (△), the solid lines indicating the best least-squares fit to the data. The combined S55D/E59G mutations leave K_1 essentially unchanged but reduce K_2 from 6.2×10^7 to 2.9×10^7 M^{-1}, resulting in a $\Delta\Delta G_{Ca}$ value of 0.5 kcal/mol. By contrast, the combined D94S/G98D mutations reduce K_1 from 2.5×10^8 to 9.7×10^7 M^{-1} and lower K_2 by more than 2 orders of magnitude to 4.4×10^5 M^{-1}, a 3.5 kcal/mol decrease in overall affinity. The α D94S/G98E variant

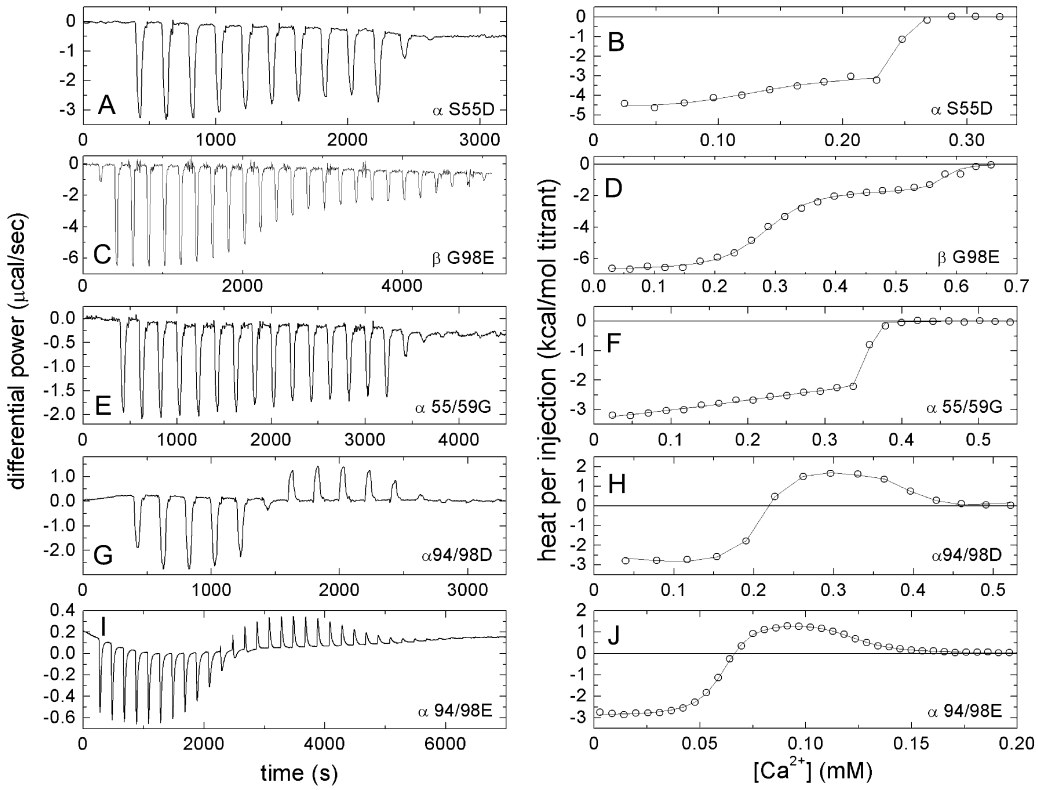

FIGURE 8: ITC analyses of Ca^{2+} binding by select α- and *β*-PV variants. (A, B) Raw and integrated data, respectively, for the titration of 130 μM α S55D with 2.5 mM Ca^{2+}. (C, D) Corresponding data for the titration of 300 μM *β* G98E with 7.5 mM Ca^{2+}. (E, F) Data for the titration of 180 μM α S55D/E59G with 5.95 mM Ca^{2+}. (G, H) Titration of 200 μM α D94S/G98D with 4.0 mM Ca^{2+}. (I, J) 2.0 mM Ca^{2+} vs 64 μM α D94S/G98E.

exhibits a comparable reduction in Ca^{2+} affinity, with macroscopic binding constants of 5.5×10^7 and 4.7×10^5 M^{-1}.

The *β* D94S/G98E variant was not included in the earlier study of the *β* site-interconversion variants (*27*). Like α D94S/G98E, it produces a substantial decrease in Ca^{2+} affinity, reducing K_1 and K_2 from 2.4×10^7 and 1.4×10^6 M^{-1} to 1.1×10^6 and 3.1×10^5 M^{-1}, respectively (Figure S1, Supporting Information). The $\Delta\Delta G_{tot}$ value of 2.7 kcal/mol is significantly larger than that measured for *β* D94S/G98D (1.9 kcal/mol).

Ca^{2+}-binding enthalpies were determined for the site-interconversion variants by ITC. Raw and integrated data are presented in Figure 8 for α S55D/E59G (panels E and F), α D94S/G98D (panels G and H), and α D94S/G98E (panels I and J). The apparent enthalpy values obtained by NLLS analysis are listed in Table 2. As shown in Figure 4, the changes in free energy of Ca^{2+} binding for these variants all include opposing enthalpy and entropy contributions. The magnitude of this enthalpy−entropy compensation is significantly larger for the 94/98 variants than for the 55/59G variants. The 94/98 variants have a major impact on ΔH and, in particular, the ΔH associated with the second equivalent of Ca^{2+}. Whereas both Ca^{2+}-binding events are exothermic in wild-type rat α, binding of the second equivalent of Ca^{2+} is endothermic in both α D94S/G98D and α D94S/G98E. In *β* D94S/G98D, both Ca^{2+}-binding events are exothermic (*27*), with ΔH_1 and ΔH_2 values of −2.8 and −0.8 kcal/mol, respectively. However, the ITC thermogram for *β* D94S/G98E, like those obtained for α D94S/G98D and α D94S/G98E, has an exothermic component and an endothermic component (Figure S1, Supporting Information). Somewhat uncharacteristically, the magnitudes of the $\Delta\Delta H$ and $-T\Delta\Delta S$ terms are larger for *β* S55D/D59G and *β* D94S/G98E than for the corresponding α variants.

DISCUSSION

Rat *β*-PV displays unusually low divalent ion affinity. In Hepes-buffered NaCl, at pH 7.4, the overall standard free energy for Ca^{2+} binding is 3.6 kcal/mol less favorable than that of rat α. In Hepes-buffered KCl, the $\Delta\Delta G$ value increases to 5.2 kcal/mol. Several years ago, we examined the consequences of (1) introducing an additional carboxylate ligand into the CD and EF site ligand arrays and (2) interconverting the ligand arrays from the two sites. Although the results were interesting, there was concern that they might be idiosyncratic for the mammalian *β* isoform. Thus, to examine the generality of these findings, the corresponding mutations have now been characterized in the rat α background. The two systems are found to yield qualitatively similar results. As illustrated by Figure 4, the changes in stability ($\Delta\Delta G_{conf}$) and overall Ca^{2+} affinity ($\Delta\Delta G_{Ca}$) are of the same sign in both systems. However, the magnitude of the alteration is typically larger for the rat α system.

Besides confirming the generality of the behavior previously observed with rat *β*, these studies furnish some insight into the relative contributions of local and remote structural determinants on EF-hand divalent ion affinity. It is apparent that the surrounding protein architecture can strongly influence the properties of a particular EF-hand ligand constellation. The discussion begins with an interesting example.

Impact of the E59D Mutation in Rat α. The $-x$ residue in the parvalbumin CD binding loop is a nearly invariant

glutamate, and the glutamyl carboxylate directly coordinates the bound Ca^{2+} ion (Figure 2B). In the rat β CD site, however, glutamate is replaced by aspartate. The aspartyl side chain cannot directly coordinate the bound ion. Instead, a water molecule serves as the proximal ligand, bridging the bound ion and the aspartyl carboxylate (Figure 2A). The attenuated Ca^{2+} affinity of the β CD site was originally attributed to this difference in coordination (*34*). Subsequently, however, replacement of Asp-59 by glutamate (D59E) was shown to have a modest impact on the metal ion-binding properties of rat β, increasing the CD site binding constant by just 20%, as judged by $^{45}Ca^{2+}$ flow dialysis (*17*, *35*).

Interestingly, the converse mutation in α, replacement of Glu-59 by aspartate, lowers the overall Ca^{2+} affinity by 1.7 kcal/mol. Converting the macroscopic constants to microscopic, or site-specific, constants, using eq 3, yields k_1 and k_2 values of 1.1×10^8 and 8.4×10^6 M^{-1}, respectively. By contrast, the two sites in wild-type α, indistinguishable in Ca^{2+}-binding assays, exhibit an average microscopic Ca^{2+}-binding constant of 1.2×10^8 M^{-1} in Hepes-buffered saline (*31*, *32*). Thus, the impact of the E59D mutation is largely confined to just one of the sites, presumably the CD site, lowering its apparent binding affinity by a factor of 14. This result, one of the more significant of this study, demonstrates that parvalbumin divalent ion affinity is coordinately influenced by the metal ion ligands and by the surrounding protein architecture. In the present case, although the identity of the $-x$ ligand in the CD site is a potentially important determinant of Ca^{2+} affinity, structural features in rat β outside of the β CD binding pocket can evidently suppress its impact.

Mutations can modify the $\Delta G^{\circ\prime}$ for Ca^{2+} binding by preferentially stabilizing the Ca^{2+}-bound state of the protein and/or by preferentially destabilizing the apoprotein. The Ca^{2+}-free α E59D variant displays increased conformational stability. The mutation raises the T_m by 4.0 deg, corresponding to a $\Delta\Delta G_{conf}$ of 0.8 kcal/mol, according to eq 4. Thus, roughly half of the $\Delta\Delta G_{Ca}$ value (1.7 kcal/mol) reflects stabilization of the unliganded state.

The remainder of the $\Delta\Delta G_{Ca}$ is presumably attributable to destabilization of the bound state. Whereas Ca^{2+} must completely shed its hydration shell in order to bind to the wild-type α CD site, it will retain a water molecule when bound in the CD site of α E59D. Retention of this water molecule should carry an entropic penalty. Assuming that the change in translational/rotational entropy accompanying immobilization of a water molecule is on the order of -5 cal mol^{-1} K^{-1} (*36*, *37*), the associated free energy penalty at 298 K would approach 1.5 kcal/mol. This value exceeds the additional 0.9 kcal/mol required to account for $\Delta\Delta G_{Ca}$. The difference could reflect the replacement of glutamate by aspartate, which would lower the conformational entropy penalty resulting from immobilization of the $-x$ side chain.

The nonreciprocal behavior of the α E59D and β D59E mutations is intriguing. Whereas α E59D lowers affinity by 1.7 kcal/mol, β D59E raises affinity by just 0.1 kcal/mol. Given that α E59D stabilizes the Ca^{2+}-free protein by 0.8 kcal/mol, one would predict that the β D59E mutation would destabilize the protein by a comparable amount. Unexpectedly, β D59E actually stabilizes the Ca^{2+}-free protein by 0.3 kcal/mol. This apparent discrepancy of 1.1 kcal/mol largely accounts for the 1.6 kcal/mol discrepancy between the predicted and observed impact of β D59E on Ca^{2+} affinity.

The explanation for the increased stability of Ca^{2+}-free β D59E is not obvious and is probably multifactorial. Conceivably, the longer side chain may permit a stabilizing interaction between the carboxylate and an adjacent basic group in the apoprotein, or the longer side chain may reduce electrostatic repulsion with neighboring anionic moieties in the Ca^{2+}-free state. Because the environment of residue 59 differs in α and β, the concept of isoform-specific electrostatic interactions appears reasonable.

Alternatively, the increased stability of β D59E may reflect increased affinity for solvent cations. Na^+ levels strongly influence the intrinsic conformational stability of rat α and β isoforms (*38*). The stabilization, the extent of which is isoform-dependent, results from binding of the monovalent ion to vacant EF-hand motifs (*32*, *38*). If the D59E substitution in β heightened the interaction with Na^+, the T_m of the Ca^{2+}-free protein should increase. Moreover, the concomitant increase in competition by Na^+ could largely nullify the anticipated entropic gain resulting from liberation of bound water from the coordination sphere. Clearly, further investigation will be required to resolve this issue.

Several other investigators have examined E → D substitutions at the $-x$ position in EF-hand systems. Franchini et al. (*39*) ascertained the consequences of the E → D substitution at the $-x$ position of a 33-residue peptide model of the carp parvalbumin CD site. They observed that replacement of glutamate by aspartate yields a 2-fold increase in Ca^{2+} affinity. Drake et al. (*40*) examined the impact of $-x$ residue identity on the quasi-EF-hand motif in the *E. coli* galactose-binding protein. They found that the Ca^{2+} affinity of Q142E ($K_d \geq 500$ μM) was much lower than that of Q142D ($K_d = 23 \pm 2$ μM), corresponding to a $\Delta\Delta G_{Ca}$ of -1.8 kcal/mol for the E142D mutation. These findings contrast strikingly with our results for the α E59D mutation, for which substitution of aspartate for glutamate causes a pronounced decrease in affinity ($\Delta\Delta G_{Ca} = 1.7$ kcal/mol).

Blumenschein and Reinach (*41*) have examined a collection of mutations at the liganding positions of site 1 in myosin regulatory light chain (RLC). When the $+z$ residue (normally aspartate) is serine and $-z$ (normally aspartate) is glutamate, as in parvalbumin, then replacement of glutamate by aspartate at $-x$ decreases Ca^{2+} affinity by a factor of 2.5 ($\Delta\Delta G_{Ca} = +0.54$ kcal/mol). This result agrees qualitatively with our data for α E59D, although the magnitude of the decrease is substantially smaller. It should be noted that, because the $+y$ residue is asparagine, rather than aspartate, in that system, the RLC variants do not perfectly mimic the parvalbumin CD site. The idiosyncratic impact seen for D ↔ E substitutions in different systems emphasizes the significance of the surrounding protein architecture.

Comparison of the α- and β-Pentacarboxylate Variants. Structure−affinity studies on EF-hand peptide models have indicated that Ca^{2+} affinity should be maximized in binding sites harboring four carboxylate ligands, aligned on the $+x$, $-x$ and $+z$, $-z$ axes (*21*−*24*). Introduction of a fifth carboxylate, in these systems, was shown to reduce metal ion affinity, presumably due to increased interligand repulsion (*25*). Thus, it was interesting to learn that the β S55D and G98D variants, which harbor five-carboxylate ligand

arrays in the CD and EF sites, respectively, exhibit heightened Ca^{2+} affinity (*26*). To probe the generality of these findings, these pentacarboxylate mutations have now been examined in the rat α background.

The *β* S55D mutation, the α S55D/E59D mutation, and the α and *β* G98D mutations all produce ligand arrays consisting of four aspartyl side chains ($+x$, $+y$, $+z$, and $-x$), a main-chain carbonyl ($-y$), and a glutamate ($-z$). The arrangement of liganding residues in these variants, in the N- to C-terminal direction, is D-D-D-(CO)-D-E, a constellation herein denoted 4DE.

Interestingly, the 4DE array does not occur naturally. Presumably, the binding properties (affinity, specificity, and kinetics) of this ligand arrangement are physiologically inappropriate. The CD site in cod *β*-parvalbumin, in which the $+z$ serine is replaced by glutamate, appears to be the closest analogue. Although Ca^{2+}-binding constants for that protein have not been reported, spectroscopic studies indicate that one of the two sites, presumably the CD site, is a low-affinity site (*42*).

The α S55D and α and *β* G98E mutations produce a ligand constellation consisting of three aspartyl side chains ($+x$, $+y$, $+z$), a backbone carbonyl ($-y$), and two glutamyl side chains ($-x$, $-z$). Thus, the arrangement of ligands, from N- to C-terminal, is D-D-D-(CO)-E-E, herein designated 3D2E.

Behavior of the 4DE Arrays. As mentioned earlier, the α E59D variant has a CD ligand array identical to that in rat *β*. When Ser-55 is replaced by aspartate in α E59D, to produce α S55D/E59D, the Ca^{2+}affinity is markedly improved. K_1 and K_2 increase by factors of 16 and 32, respectively, yielding an overall $\Delta\Delta G_{Ca}$ value of −3.7 kcal/mol.

Relative to wild-type α, K_1 and K_2 in α S55D/E59D are increased by factors of 7.3 and 3.9, respectively, for a $\Delta\Delta G_{Ca}$ of −2.0 kcal/mol. The corresponding Mg^{2+} constants are increased by factors of 15 and 4.4 ($\Delta\Delta G_{Mg}$ of −2.5 kcal/mol).

Replacement of Gly-98 by aspartate, to produce α G98D, also raises Ca^{2+} affinity, albeit to a lesser extent. K_1 and K_2 increase by factors of 4.6 and 1.2, respectively ($\Delta\Delta G_{Ca}$ value of −1.0 kcal/mol). The Mg^{2+} binding constants exhibit relatively smaller changes. K_{1M} increases by approximately 75%, but K_{2M} decreases by roughly 20%, for a $\Delta\Delta G_{Mg}$ of −0.2 kcal/mol.

These results are qualitatively similar to those obtained previously with rat *β* (*26*). In that system, the S55D and G98D mutations were found to improve overall Ca^{2+} affinity by 1.7 and 1.3 kcal/mol, respectively, and whereas *β* S55D heightened overall Mg^{2+} affinity by 3.2 kcal/mol, *β* G98D yielded a $\Delta\Delta G_{Mg}$ of just −0.2 kcal/mol. The much smaller impact of the G98D mutation on Mg^{2+} affinity was also apparent in DSC studies on the *β* variants in the presence of 20 mM Mg^{2+}. Whereas S55D raised the T_m by 10.5 deg, G98D raised it by a mere 0.5 deg.

It would appear, then, that mutations producing the 4DE array exert a greater impact in the CD site, elevating both Ca^{2+} and Mg^{2+} affinities. The same mutations in the EF site afford a smaller increase in Ca^{2+} affinity and leave Mg^{2+} affinity essentially unchanged.

In their investigation of mutations within myosin RLC site I, Blumenshein and Reinach (*41*) observed that the Ca^{2+}- and Mg^{2+}-binding constants for the D12E variant are increased by factors of 10 and 8.5, respectively, relative to the D5S/D12E variant. Except for the replacement of aspartate by asparagine at $-y$ alluded to earlier, the ligation in RLC D12E mimics that in *β* S55D, and RLC D5S/D12E mimics the wild-type *β* CD site. Thus, the results obtained in the RLC system are consistent with the findings in rat α and *β*.

Although mutations producing pentacarboxylate arrays significantly increase Ca^{2+} affinity, the enthalpic and entropic contributions differ between the CD and EF sites and between α and *β*. As shown in panels C and D of Figure 6, the enthalpic gains that accompany the CD loop mutations (α S55D/E59D and *β* S55D) are larger than those accompanying the G98D mutations in the EF site. The enthalpic improvement in α S55D/E59D, but not *β* S55D, is offset somewhat by a compensatory entropic change. Although α and *β* G98D variants display similar increases in Ca^{2+} affinity, they differ in the thermodynamic details. The more favorable $\Delta\Delta G_{Ca}$ for α G98D reflects an enthalpic gain and includes a compensatory entropic contribution. By contrast, the $\Delta\Delta H_{Ca}$ measured for *β* G98D is negligible, and the negative $\Delta\Delta G_{Ca}$ is entirely entropic.

All of the mutations that yield a 4DE array significantly destabilize the Ca^{2+}-free protein. The T_m shift is larger for the mutations involving the CD site (−8.5° for α S55D/E59D, −4.3° for *β* S55D) than for those involving the EF site (−2.6° for α G98D, −1.8° for *β* G98D). This difference may reflect the difference in placement of the two binding loops. Positioned near the C-terminus, the EF site can presumably undergo minor conformational rearrangements, to reduce electrostatic repulsion, without involving the remainder of the molecule. By contrast, conformational changes in the CD site, located in the middle of the sequence, will require compensatory movements in the adjacent protein structure.

The larger ΔT_m values are consistent with the more negative $\Delta\Delta H_{Ca}$ changes observed for the mutations in the CD binding loop. The lower melting temperatures suggest that the proteins may be less tightly folded in the apo form, so that Ca^{2+} binding produces a greater increase in van der Waals contacts and consequently greater exothermicity.

As noted above, mutations can alter the free energy change for Ca^{2+} binding by preferentially stabilizing the Ca^{2+}-bound state of the protein or preferentially destabilizing the Ca^{2+}-free state. The previous analysis of *β* S55D and *β* G98D (*26*) suggested that destabilization of the apo form contributes significantly to the increase in divalent ion affinity observed for these proteins. The data obtained on α S55D/E59D and α G98D reinforce this conclusion. For example, the overall $\Delta G°'$ for Ca^{2+} binding is 2.0 kcal/mol more favorable for α S55D/E59D than for wild-type α. As the data in Table 1 suggest, approximately 1.7 kcal/mol of that quantity results from destabilization of the Ca^{2+}-free protein. The $\Delta G°'$ for Ca^{2+} binding is 3.7 kcal/mol more favorable, relative to α E59D, approximately 3.0 kcal/mol of which is attributable to the reduced stability of the Ca^{2+}-free protein. The suggestion that 70% or more of the $\Delta\Delta G_{Ca}$ value reflects energetic alterations in the apoprotein serves as a reminder that unliganded and liganded forms can both influence binding equilibria.

Roughly 0.3 kcal/mol of the 2.0 kcal/mol increase in Ca^{2+} affinity for α S55D/E59D, relative to wild-type α, can be

attributed to increased stability of the bound protein. Recently acquired structural data for α S55D/E59D reveals that the Asp-59 carboxylate does not participate in Ca^{2+} coordination (Y.-H. Lee, J. D. Larson, M. T. Henzl, and J. J. Tanner, unpublished data). Instead, it has rotated approximately 90°, assuming a position well suited for stabilizing the D helix dipole. This helix-capping interaction may underlie the apparent increase in the stability of the Ca^{2+}-bound protein.

Behavior of the 3D2E Array. Three of the variants described here possess a 3D2E ligand constellation: the α S55D variant and the α and β G98E variants. α S55D produces a slight reduction in both K_1 and K_2, to 2.1×10^8 and 5.0×10^7 M^{-1}, respectively ($\Delta\Delta G_{Ca} = 0.2$ kcal/mol). On the other hand, α G98E yields values of K_1 and K_2 of 4.4×10^8 and 5.3×10^7 M^{-1}, a slight improvement in overall Ca^{2+} affinity ($\Delta\Delta G_{Ca} = -0.2$ kcal/mol). The β variant exhibits a comparable alteration.

As in the 4DE variants, the 3D2E variants strongly destabilize the Ca^{2+}-free protein. In α, the S55D and G98E mutations lower the conformational stability by 2.2 and 2.7 kcal/mol, respectively. Unlike their 4DE counterparts, however, destabilization of the apoprotein does not produce large increases in divalent ion affinity. Presumably, then, α S55D and the α and β G98E mutations cause comparable destabilization of the Ca^{2+}-bound form of the protein as well. Structural analysis of a representative variant, currently in progress, may furnish insight into this issue.

Comparison of the α and β Site-Interconversion Variants. These variants were originally prepared in rat β to assess the relative importance of ligand identity and context on the performance of the CD and EF ligand arrays (*27*). As with the pentacarboxylate variants, the corresponding mutations have been prepared and characterized in the α isoform background, to assess the generality of the earlier findings.

The results of the site-interconversion studies in the two isoforms are consistent. Wild-type parvalbumin EF sites exhibit a high-affinity phenotype. However, when the EF site ligand array is imported into the CD binding loop, the array exhibits behavior qualitatively similar to that of the wild-type CD site. Whereas it acquires a low-affinity signature in the β isoform (β S55D/D59G), in the α isoform (α S55D/E59G), it remains a high-affinity site. These results attest to the strong influence of the overall environment of the CD site as a determinant of ion-binding affinity, superseding the intrinsic ion-binding behavior of a particular array. Moreover, they provide additional evidence that the anomalously low affinity of the mammalian β CD site is a consequence of higher order structural considerations.

By contrast, when the CD site ligand array, a low-affinity array in β and a high-affinity array in α, is imported into the EF binding loop, it exhibits a low-affinity signature. This result is likewise obtained when the α ligand array is placed in the β EF binding loop (β D94S/G98E) and, conversely, when the β ligand array is placed in the α EF loop (α D94S/G98D).

Although the D94S/G98D and D94S/G98E variants exhibit uniformly low affinity for Ca^{2+}, they differ in their impact on apoprotein stability. The combined D94S and G98D mutations stabilize the Ca^{2+}-free protein ($\Delta T_m = 5.4°$ and $\Delta\Delta G_{conf} = 1.1$ kcal/mol for α; $\Delta T_m = 1.4°$ and $\Delta\Delta G_{conf} = 0.3$ kcal/mol for β). By contrast, the combined D94S and G98E mutations destabilize the protein (ΔT_m of $-3.3°$ and $\Delta\Delta G_{conf} = -0.6$ kcal/mol for α; ΔT_m of $-1.2°$ and $\Delta\Delta G_{conf} = -0.3$ kcal/mol for β). The disparate impact on stability suggests that the longer glutamyl side chain at $-x$ in D94S/G98E increases repulsion in the apoprotein. Interestingly, however, despite the 1.7 kcal/mol difference in conformational stability, α D94S/G98D and α D94S/G98E differ in total binding free energy by just a mere 0.3 kcal/mol. This disparity suggests that the electrostatic cost attendant to the replacement of Asp-98 with glutamate may be offset by the more complete dehydration of the bound Ca^{2+}. As noted earlier, the entropic benefit associated with the release of a bound water molecule could be on the order of 1.5 kcal/mol.

Whereas α D94S/G98D and α D94S/G98E differ by only 0.3 kcal/mol in Ca^{2+} affinity, the corresponding β variants differ by 0.8 kcal/mol, one of the few examples in this study of a larger $\Delta\Delta G$ value for the β system. Although the reason for the larger difference in affinity is not understood, we note that β D94S/G98D and β D94S/G98E also exhibit distinct enthalpic signatures for Ca^{2+} binding. The titrations of both α variants display an initial exothermic binding event, followed by an endothermic component (Figure 10, panels H and I). However, only the D94S/G98E variant shows this behavior in β. Both Ca^{2+}-binding events in β D94S/G98D are exothermic. In consequence, whereas β 94/98D exhibits a $\Delta\Delta H_{Ca}$ value of 4.0 kcal/mol, the corresponding value for β 94/98E is 6.6 kcal/mol.

Clearly, the CD site ligand array undergoes a marked reduction in Ca^{2+} affinity when placed in the context of the EF site. This finding might indicate that the CD ligand array has intrinsically lower affinity for Ca^{2+} than the EF array or that the CD site ligand geometry may not be well suited to the EF site environment, proximal to the C-terminus. Alternatively, the parvalbumin fold may not be able to accommodate the juxtaposition of two CD ligand arrays. The CD and EF binding loops are joined by a short segment of antiparallel β structure, which allows for cooperative interactions between the two sites. The presence of the CD-like ligand array in the EF binding loop may subtly alter the path of the peptide chain, weakening the hydrogen bonds in the β segment. Although typical parvalbumin CD and EF sites behave equivalently in divalent ion-binding assays, there is a strongly positive interaction between them (*32*). Perturbation of the β-structure linking the two sites could reduce the degree of cooperativity, causing a marked reduction in the affinity of the weaker site. High-resolution structural data for one of these variants might clarify this issue.

CONCLUDING REMARKS

We have examined the behavior of the pentacarboxylate and site-interconversion variants in two very different parvalbumin backgrounds. The pentacarboxylate ligand array places aspartyl residues at $+x$, $+y$, $+z$, and $-x$. This ligand constellation exhibits similar behavior in rat α and β. When the mutations are made in the CD site (to produce either α S55D/E59D or β S55D), Ca^{2+} and Mg^{2+} affinity both increase substantially. When the mutations are made in the EF site (to produce either α or β G98D), the impact on overall Ca^{2+} affinity is somewhat smaller, although still significant, and overall Mg^{2+} affinity is little changed. In all four variants, the increase in divalent ion affinity results primarily from destabilization of the apoprotein.

The parvalbumin EF site exhibits a high-affinity phenotype in both α and β. However, when placed in the context of the CD site, its behavior is isoform-dependent. Inserted into the high-affinity α CD site, it exhibits a high-affinity signature; inserted into the low-affinity β CD site, it exhibits a low-affinity signature. This finding suggests that the environment of the CD site exerts a strong influence on the divalent ion-binding properties of the resident ligand array.

By contrast, when the CD site ligand array, from either α or β, is placed in the context of the EF site, in either α or β, Ca^{2+} affinity drops precipitously. The physical basis for the reduction in affinity is presently uncertain. Optimal performance of this ligand array may conceivably require the more rigid CD site scaffold. Alternatively, the presence of two CD site ligand constellations may not be entirely compatible with the parvalbumin tertiary structure.

With few exceptions, the mutations described here produce qualitatively similar perturbations in both rat α and β. In general, however, the absolute magnitudes of the changes are larger in the α background. This trend, particularly evident in the observed ΔT_m and $\Delta\Delta G_{conf}$ values, suggests that the structure of α may be more malleable, or less rigid, than that of β.

Above all, these data reinforce the idea that context strongly influences the performance of a given EF-hand ligand array. Although the pentacarboxylate arrays exhibit reduced divalent ion affinity in model peptide systems, they show heightened affinity in the context of a fully folded parvalbumin molecule. The wild-type EF site ligand array behaves as either a high- or a low-affinity site, depending upon whether it is placed in the context of the α or β CD site, respectively. Regardless of its behavior in the wild-type CD site, the CD array adopts a low-affinity signature when placed in the context of the EF binding loop. Finally, the identity of the $-x$ residue, whether aspartate or glutamate, has little influence on the Ca^{2+} affinity of the rat β CD site. However, replacement of the $-x$ glutamate by aspartate has a major impact on the Ca^{2+} affinity of rat α. Evidently, the functional characteristics of a particular array can be strongly modulated by the surrounding protein environment.

SUPPORTING INFORMATION AVAILABLE

Figure S1 presents raw and integrated ITC data for the titration of β D94S/G98E with Ca^{2+}. This material is available free of charge via the Internet at http://pubs.acs.org.

REFERENCES

1. Berridge, M. J. (1997) Elementary and global aspects of calcium signaling, *J. Physiol. 499*, 291−306.
2. Kretsinger, R. H. (1980) Structure and evolution of calcium modulated proteins, *CRC Crit. Rev. Biochem. 8*, 115−164.
3. Celio, M. R., Pauls, T., and Schwaller, B. (1996) *Guidebook to the Calcium-Binding Proteins*, Oxford University Press, New York.
4. Seamon, K. B., and Kretsinger, R. H. (1983) Calcium-modulated proteins, in *Calcium in Biology* (Spiro, T. G., Ed.) pp 3−51, John Wiley and Sons, New York.
5. Falke, J. J., Drake, S. K., Hazard, A. L., and Peersen, O. B. (1994) Molecular tuning of ion binding to calcium signaling proteins, *Q. Rev. Biophys. 27*, 219−290.
6. Linse, S., and Forsen, S. (1995) Determinants that govern high-affinity calcium binding, *Adv. Second Messenger Phosphoprotein Res. 30*, 89−151.
7. Wnuk, W., Cox, J. A., and Stein, E. A. (1982) Parvalbumins and other soluble high-affinity calcium-binding proteins from muscle, in *Calcium and Cell Function* (Cheung, W. Y., Ed.) Vol. 2, pp 243−278, Academic Press, New York.
8. Pauls, T. L., Cox, J. A., and Berchtold, M. W. (1996) The Ca^{2+}-binding proteins parvalbumin and oncomodulin and their genes: new structural and functional findings, *Biochim. Biophys. Acta 1306*, 39−54.
9. Ahmed, F. R., Rose, D. R., Evans, S. V., Pippy, M. E., and To, R. (1993) Refinement of recombinant oncomodulin at 1.30 Å Resolution, *J. Mol. Biol. 230*, 1216−1224.
10. Kretsinger, R. H., and Nockolds, C. E. (1973) Carp muscle calcium-binding protein. II. Structure determination and general description, *J. Biol. Chem. 248*, 3313−3326.
11. Goodman, M., and Pechére, J.-F. (1977) The evolution of muscular parvalbumins investigated by the maximum parsimony method, *J. Mol. Evol. 9*, 131−158.
12. Nakayama, S., Moncrief, N. D., and Kretsinger, R. H. (1992) Evolution of EF-hand calcium-modulated proteins. II. Domains of several subfamilies have diverse evolutionary histories, *J. Mol. Evol. 34*, 416−448.
13. Fohr, U. G., Weber, B. R., Muntener, M., Staudenmann, W., Hughes, G. J., Frutiger, S., Banville, D., Schafer, B. W., and Heizmann, C. W. (1993) Human alpha and beta parvalbumins. Structure and tissue-specific expression, *Eur. J. Biochem. 215*, 719−727.
14. Rinaldi, M. L., Haiech, J., Pavlovitch, J., Rizk, M., Ferraz, C., Derancourt, J., and Demaille, J. G. (1982) Isolation and characterization of a rat skin parvalbumin-like calcium-binding protein, *Biochemistry 21*, 4805−4810.
15. Pauls, T. L., Durussel, I., Cox, J. A., Clark, I. D., Szabo, A. G., Gagne, S. M., Sykes, B. D., and Berchtold, M. W. (1993), Metal binding properties of recombinant rat parvalbumin wild-type and F102W mutant, *J. Biol. Chem. 268*, 20897−20903.
16. Eberhard, M., and Erne, P. (1994) Calcium and magnesium binding to rat parvalbumin, *Eur. J. Biochem. 222*, 21−26.
17. Hapak, R. C., Lammers, P. J., Palmisano, W. A., Birnbaum, E. R., and Henzl, M. T. (1989) Site-specific substitution of glutamate for aspartate at position 59 of rat oncomodulin, *J. Biol. Chem. 264*, 18751−18760.
18. Cox, J. A., Milos, M., and MacManus, J. P. (1990) Calcium- and magnesium-binding properties of oncomodulin, *J. Biol. Chem. 265*, 6633−6637.
19. Epstein, P., Means, A. R., and Berchtold, M. W. (1986) Isolation of a rat parvalbumin gene and full length cDNA, *J. Biol. Chem. 261*, 5886−5891.
20. Gillen, M. F., Banville, D., Rutledge, R. G., Narang, S., Seligy, V. L., Whitfield, J. F., and MacManus, J. P. (1987) A complete complementary DNA for the oncodevelopmental calcium-binding protein, oncomodulin, *J. Biol. Chem. 262*, 5308−5312.
21. Reid, R. E., and Hodges, R. S. (1980) Co-operativity and calcium/magnesium binding to troponin C and muscle calcium binding parvalbumin: an hypothesis, *J. Theor. Biol. 84*, 401−444.
22. Reid, R. E. (1990) Synthetic fragments of calmodulin calcium-binding site III. A test of the acid pair hypothesis, *J. Biol. Chem. 265*, 5971−5976.
23. Procyshyn, R. M., and Reid, R. E. (1994) A structure/activity of calcium affinity and selectivity using a synthetic peptide model of the helix-loop-helix calcium-binding motif, *J. Biol. Chem. 269*, 1641−1647.
24. Procyshyn, R. M., and Reid, R. E. (1994) An examination of glutamic acid in the $-x$ chelating position of the helix-loop-helix calcium binding motif, *Arch. Biochem. Biophys. 311*, 425−429.
25. Marsden, B. J., Hodges, R. S., and Sykes, B. D. (1988) ^{1}H NMR Studies of synthetic peptide analogues of calcium-binding site III of rabbit skeletal troponin C: Effect on the lanthanum affinity of the interchange of aspartic acid and asparagines residues at the metal ion coordinating positions, *Biochemistry 27*, 4198−4206.
26. Henzl, M. T., Hapak, R. C., and Goodpasture, E. A. (1996) Introduction of fifth carboxylate ligand heightens affinity of the oncomodulin CD and EF sites for Ca^{2+}, *Biochemistry 35*, 5856−5869.
27. Henzl, M. T., Hapak, R. C., and Likos, J. J. (1998) Interconversion of the ligand arrays in the CD and EF sites of oncomodulin. Influence on Ca^{2+}-binding affinity, *Biochemistry 37*, 9101−9111.
28. Henzl, M. T., and Graham, J. S. (1999) Conformational stabilities of the rat α- and β-parvalbumins, *FEBS Lett. 442*, 241−245.
29. Henzl, M. T., Agah, S., and Larson, J. D. (2003) Characterization of the metal ion-binding domains from rat α- and β-parvalbumins, *Biochemistry 42*, 3594−3607.

30. Womack, F. C., and Colowick, S. P. (1973) Rapid measurement of binding of ligands by rate of dialysis, *Methods Enzymol. 27*, 464−471.
31. Henzl, M. T., Larson, J. D., and Agah, S. (2003) Estimation of parvalbumin Ca^{2+}- and Mg^{2+}-binding constants by global least squares analysis of isothermal titration calorimetry data, *Anal. Biochem. 319*, 216−233.
32. Henzl, M. T., Larson, J. D., and Agah, S. (2004) Influence of monovalent cation identity on parvalbumin divalent ion-binding properties, *Biochemistry 43*, 2747−2763.
33. Bechtel, W. J., and Schellman, J. A. (1987) Protein stability curves, *Biopolymers 26*, 1859−1877.
34. Williams, T. C., Corson, D. C., Sykes, B. D., and MacManus, J. P. (1987) Oncomodulin. ^1H NMR and optical stopped-flow spectroscopic studies of its solution conformation and metal-binding properties, *J. Biol. Chem. 262*, 6248−6256.
35. Palmisano, W. A., Trevino, C. L., and Henzl, M. T. (1990) Site-specific replacement of amino acid residues within the CD binding loop of rat oncomodulin, *J. Biol. Chem. 265*, 14450−14456.
36. Amzel, M. (1997) Loss of translational entropy in binding, folding, and catalysis, *Proteins 29*, 1−6.
37. Tamura, A., and Privalov, P. L. (1997) The entropy cost of protein association, *J. Mol. Biol. 273*, 1048−1060.
38. Henzl, M. T., Larson, J. D., and Agah, S. (2000), Influence of monovalent cations on rat α- and β-parvalbumin stabilities, *Biochemistry 39*, 5859−5867.
39. Franchini, P. L., and Reid, R. E. (1999) Investigating site-specific effects of the -x glutamate in a parvalbumin CD site model peptide, *Arch. Biochem. Biophys. 372*, 80−88.
40. Drake, S. K., Lee, K. L., and Falke, J. J. (1996) Tuning the equilibrium ion affinity and selectivity of the EF-hand Ca^{2+}-binding motif: substitutions at the gateway residue, *Biochemistry 35*, 6697−6705.
41. Blumenshein, T. M. A., and Reinach, F. C. (2000) Analysis of affinity and specificity in an EF-hand site using double mutant cycles, *Biochemistry 39*, 3606−3610.
42. Hutnik, C. M., MacManus, J. P., and Szabo, A. G. (1990) A calcium-specific conformational response of parvalbumin, *Biochemistry 29*, 7318−7328.

BI049582D